pubs.acs.org/acschemicalbiology

Articles

Exploiting the Cullin E3 Ligase Adaptor Protein SKP1 for Targeted Protein Degradation

Seong Ho Hong, Anand Divakaran, Akane Osa, Oscar W. Huang, Ingrid E. Wertz, and Daniel K. Nomura*

Cite This: https://doi.org/10.1021/acschembio.3c00642

Read Online

ACCESS | Metrics & More | Article Recommendations | Supporting Information

ABSTRACT: Targeted protein degradation with proteolysis targeting chimeras (PROTACs) is a powerful therapeutic modality for eliminating disease-causing proteins through targeted ubiquitination and proteasome-mediated degradation. Most PROTACs have exploited substrate receptors of Cullin-RING E3 ubiquitin ligases such as cereblon and VHL. Whether core, shared, and essential components of the Cullin-RING E3 ubiquitin ligase complex can be used for PROTAC applications remains less explored. Here, we discovered a cysteine-reactive covalent recruiter EN884 against the SKP1 adapter protein of the SKP1-CUL1-F-box containing the SCF complex. We further showed that this recruiter can be used in PROTAC applications to degrade neo-substrate proteins such as BRD4 and the androgen receptor in a SKP1- and proteasome-dependent manner. Our studies demonstrate that core and essential adapter proteins within the Cullin-RING E3 ubiquitin ligase complex can be exploited for targeted protein degradation applications and that covalent chemoproteomic strategies can enable recruiter discovery against these targets.

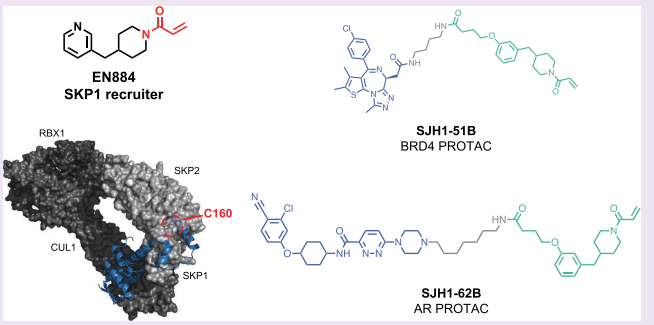

INTRODUCTION

Targeted protein degradation with heterobifunctional Proteolysis targeting chimeras (PROTACs) consisting of a protein-targeting ligand linked to E3 ubiquitin ligase recruiters has emerged as a powerful therapeutic modality for degrading disease-causing proteins through proteasome-mediated degradation. While there are >600 E3 ligases, most PROTACs have utilized a small number of E3 ligases for recruitment including cereblon and Von Hippel-Lindau (VHL).[1−4] Many additional recruiters have been discovered in recent years against additional E3 ligases, including cIAP, MDM2, DCAF16, DCAF11, RNF114, RNF4, FEM1B, KEAP1, and DCAF1.[5−16] While some of these E3 ligases are essential for cancer cell viability, many of them are not, and as such, resistance mechanisms can potentially arise in cancer cells that impair E3 ligase recruitment and render the PROTAC ineffective.[17−19] Developing recruiters against core components of the ubiquitin-proteasome machinery, such as against Cullin-RING E3 ligase complex adaptor proteins including DDB1, SKP1, or ELOB/ELOC in CUL1-CUL7 E3 ligases that are essential to cell viability, may avoid potential future resistance mechanisms that may arise from PROTACs.[17,18,20] We chose to focus here on adapter proteins of Cullin-RING E3 ligases since these adapter proteins serve as the interface for hundreds of E3 ligase substrate receptors. As such, they are particularly essential to cell viability since their elimination or dysfunction would result in impaired functions of many E3 ligase substrate receptors.

Recruitment of Cullin-RING E3 ligase adaptor proteins for targeted protein degradation has precedence. Slabicki et al. discovered that a cyclin-dependent kinase inhibitor CR8 degrades cyclin K through acting as a molecular glue between CDK12-cyclin K and the CUL4 adaptor protein DDB1.[21] Various viruses have also co-opted adaptor proteins within Cullin-RING E3 ligase complexes. For example, the human papilloma virus (HPV) E7 protein is responsible for host cellular oncogenic transformation and co-opts Elongin C in the CUL2 complex to ubiquitinate and degrade the RB tumor suppressor.[22] Paramyxovirus and Simian Virus 5 V proteins both co-opt the CUL4 adaptor protein DDB1.[22] We have also recently discovered a covalent DDB1 recruiter that can be exploited for PROTAC applications.[23]

Given our previous success in targeting the CUL4 adaptor protein DDB1 for PROTAC applications, we decided to focus on another Cullin adaptor protein. Among them, we had previously identified that C160 appeared to be a particularly

Received: October 20, 2023
Revised: January 12, 2024
Accepted: January 18, 2024

Downloaded via UNIV OF CALIFORNIA BERKELEY on February 2, 2024 at 15:48:10 (UTC).
See https://pubs.acs.org/sharingguidelines for options on how to legitimately share published articles.

ACS Publications © XXXX American Chemical Society

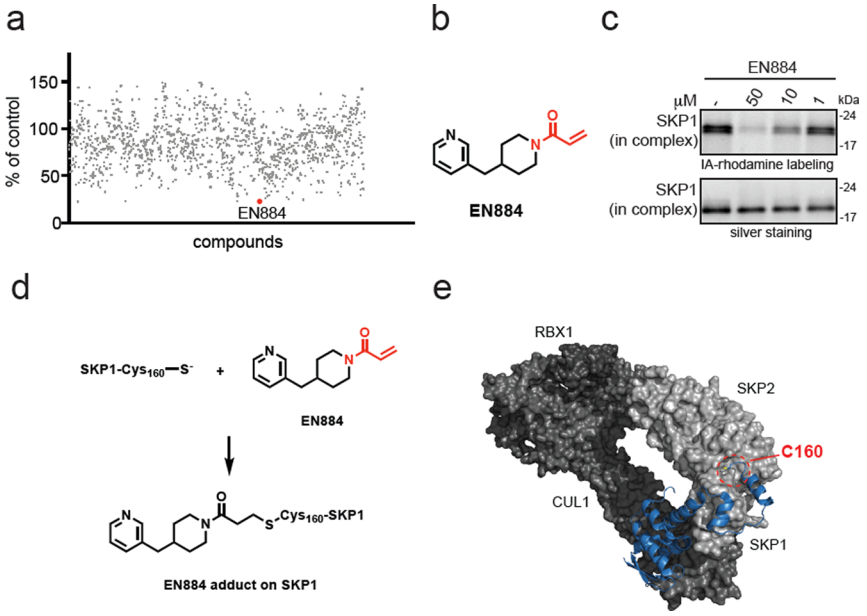

Figure 1. Discovery of a covalent SKP1 recruiter. (a) Gel-based ABPP screening of a cysteine-reactive covalent ligand library (50 μM) against a rhodamine-functionalized iodoacetamide (IA-rhodamine) labeling of pure SKP1 protein in the SKP1-FBXO7-CUL1-RBX1 complex. Individual compound values are noted as percent of labeling compared to that of DMSO vehicle control. EN884 was the top hit that showed the most inhibition of probe labeling. Structures of compounds screened and screening data can be found in Table S1. (b) Structure of EN884 with the cysteine-reactive acrylamide warhead in red. (c) Gel-based ABPP of EN884 competition against IA-rhodamine labeling. Pure SKP1 in the SKP1-FBXO7-CUL1-RBX1 complex was preincubated with EN884 1 h prior to labeling with IA-rhodamine (100 nM) for 30 min after which the proteins were separated by SDS/PAGE and visualized by in-gel fluorescence. Protein loading was assessed by silver staining. (d) Mass spectrometry analysis of EN884 modification on SKP1 shown in Figure S2a within the SKP1-FBXO7-CUL1-RBX1 complex from incubation of the complex with EN884 (50 μM) for 1 h, followed by MS/MS analysis of tryptic digests revealed one site of EN884 modification on SKP1 at C160. (e) Shown is the location in the circle of SKP1 C160 in the CUL1 complex with SKP1 in blue, in complex with SKP2, RBX1, and CUL1. Shown is an SCF complex model derived from superimposing the crystal structures of Skp1-Skp2-Cks1 with p27 peptide (PDB ID: 2AST) and Cul1-Rbx1-Skp1-Skp2 (PDB ID: 1LDK). SKP1 is shown as the blue ribbon structure, SKP2 in light gray, and RBX1-CUL1 in dark gray. The C160 side-chain is shown in yellow and circled in red. Data shown in (b) are from n = 3 biologically independent replicates per group.

aberrantly reactive cysteine within SKP1 from aggregate cysteine chemoproteomic profiling and mining for potential reactive cysteines within the ubiquitin-proteasome system, suggesting that this site may be tractable for covalent targeting and recruitment.[1] As such, we investigated whether the CUL1-RING E3 ligase adaptor protein SKP1 could be recruited for PROTAC-mediated degradation of neo-substrates. We used covalent chemoproteomic approaches to discover a SKP1 recruiter that can be used for PROTACs to degrade neo-substrates in cells.

RESULTS

Discovering a Covalent Recruiter Against SKP1. We sought to identify a covalent binder for SKP1. We screened 1284 cysteine-reactive covalent ligands in a gel-based activity-based protein profiling (ABPP) screen competing covalent ligands against a fluorophore-conjugated cysteine-reactive iodoacetamide probe (IA-rhodamine) labeling of pure human SKP1-FBXO7-CUL1-RBX1 complex (Figures 1a; S1; Table S1).[14,24] The CUL1-SKP1-RBX1 complex is shared across many of the Cullin-RING E3 ligase families, and FBXO7 represents a representative CUL1 E3 ligase substrate receptor that is commercially available.[20] The covalent ligand library consisted of covalent fragments bearing cysteine-reactive acrylamide and chloroacetamide warheads that were hand-picked for structural diversity and purchased from Enamine. We subsequently repurchased and retested any resulting hit compounds from the initial screen. The top reproducible hit that arose from this screen was EN884 that showed dose–responsive displacement of cysteine-reactive probe labeling of pure human SKP1 protein in the SKP1-FBXO7-CUL1-RBX1 complex (Figure 1b,c). We next performed tandem mass spectrometry (MS/MS) analysis on the SKP1-FBXO7-CUL1-RBX1 complex incubated with EN884 to identify the site of modification. We identified one site that was modified—C160 on SKP1 (Figures 1d; S2a). C160 resides at the C-terminus of SKP1, a region that is predicted to be an intrinsically disordered region (IDR) of the protein (Figure S2b). Previous studies have indicated that its conformational flexibility plays a pivotal role in SKP1 interaction with various F-Box domains characterized by diverse sequences and structures.[25−29] Consequently, the C-terminus of SKP1 adopts a unique conformation contingent upon its interaction with specific F-Box domains (Figures 1e; S3). Thus, we hypothesize that our covalent SKP1 recruiters may exploit and bind in between the collective interfaces between SKP1 and CUL1 substrate receptors. While structural information on FBXO7 remains elusive, analyses of representative and structurally resolved SKP1 − F-box domain protein complexes, such as SKP2, FBG3, FBXW7, or FBXO2, suggests that perhaps EN884 engages only a subset of SKP1 protein engaged with specific CUL1 substrate receptors (Figures 1e; S3). These representative examples were chosen to show the position of C160 within fully assembled CUL1 E3 ligase complexes.

During our efforts to generate alkyne-functionalized probes and heterobifunctional degraders exploiting the EN884

https://doi.org/10.1021/acschembio.3c00642
ACS Chem. Biol. XXXX, XXX, XXX−XXX

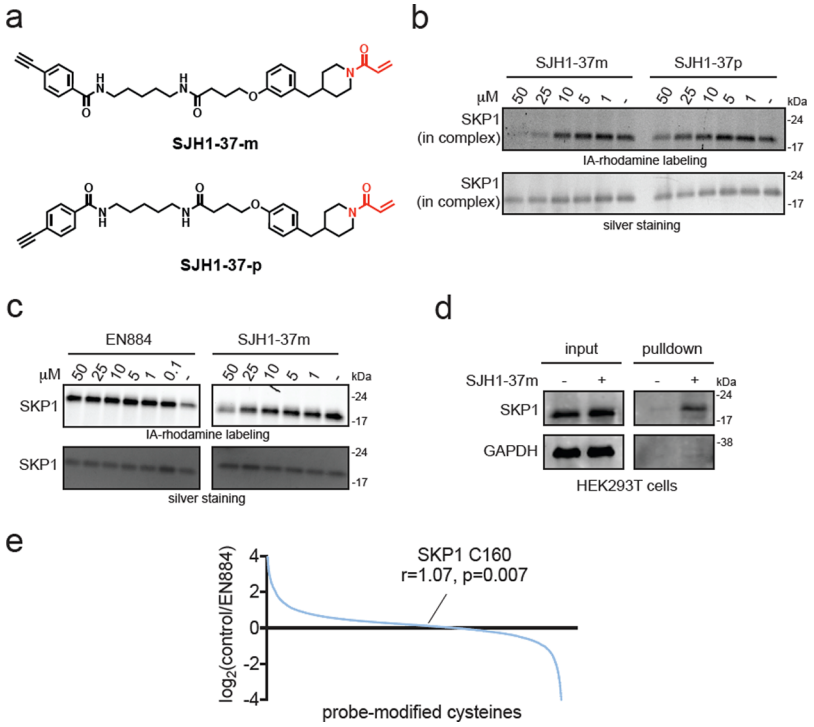

Figure 2. Characterization of covalent SKP1 recruiter. (a) Structures of two alkyne-functionalized probes based on EN884. (b) Gel-based ABPP of both probes against IA-rhodamine labeling of pure SKP1 in the SKP1-FBXO7-CUL1-RBX1 complex as described in (a). (c) Gel-based ABPP of EN884 and SJH1−37m against pure SKP1 not in complex. (d) SKP1 pulldown using SJH1−37m probe. HEK293T cells were treated with DMSO vehicle or SJH1−37m (50 μM) for 4 h. Lysates were subjected to copper-catalyzed azide−alkyne cycloaddition (CuAAC) to append on a biotin enrichment handle after which probe-modified proteins were avidin-enriched and separated on SDS/PAGE, and SKP1 and an unrelated protein GAPDH were detected by Western blotting. (e) isoDTB-ABPP analysis of EN884 in HEK293T cells. HEK293T cells were treated with DMSO vehicle or EN884 (50 μM) for 4 h, after which lysates were labeled with an alkyne-functionalized iodoacetamide probe (IA-alkyne), and control and treated cells were subjected to CuAAC with a desthiobiotin-azide with an isotopically light or heavy handle, respectively. After the isoDTB-ABPP procedure, probe-modified peptides were analyzed by LC-MS/MS, and control vs treated probe-modified peptide ratios were quantified. Chemoproteomic data can be found in Table S2. Data shown in (b, c, d, e) are from n = 3 biologically independent replicates per group.

scaffold, we encountered synthetic challenges extending off the pyridine ring. As such, we explored the impact of replacing the pyridine ring on EN884 with benzene. We thus generated AD-5−49, an EN884 analogue bearing a benzene ring instead of a pyridine (Figure S4a). This molecule was still capable of binding to SKP1 in the Cullin complex comparably to EN884 as assessed by gel-based ABPP (Figure S4a). Toward better understanding structure−activity relationships and optimal exit vector for generating probes and PROTACs, we generated AD-5−49 analogues AD-5−47a and AD-5−47b bearing methoxy substituents at either the *meta*- or *para*-position, respectively (Figure S4a). Interestingly, while AD-5−47a with the *meta*-methoxy substituent showed binding to SKP1 in the Cullin complex, AD-5−47b with the *para*-methoxy substituent showed less binding to SKP1 (Figure S4a). AD-5−49, AD-5−47a, and AD-5−47b were not able to bind to SKP1 alone (Figure S4b). Overall, these data indicated that the pyridine nitrogen was dispensable for SKP1 binding and that extension off the benzene ring at the *meta*-position was more favored.

We next synthesized two alkyne-functionalized probes based on AD-5−49 with either exit vectors off either the *meta* or *para*-position of the phenyl ring to yield SJH1−37m or SJH1−37p, respectively (Figure 2a). Based on gel-based ABPP assessment of binding of each of these probes to the SKP1 complex, the *meta*-position was once again significantly more favored compared to *para* (Figure 2b). Interestingly, and consistent with the position of C160 on SKP1 interfacing with CUL1 substrate receptors, EN884 and SJH1−37m did not bind or bound weaker to monomeric SKP1 compared to SKP1 in the complex (Figure 2c). These results demonstrated that the rest of the CUL1 complex, or at least the substrate receptor, was required for ligand binding to SKP1. We further showed that SJH1−37m engages SKP1 in cells through pulldown of SKP1, but not unrelated proteins such as GAPDH, from probe treatment and subsequent appendage of a biotin enrichment handle by copper-catalyzed azide−alkyne cycloaddition (CuAAC) and avidin-enrichment (Figure 2d). We next performed mass spectrometry-based ABPP to identify the cysteine engaged in SKP1 by EN884 in HEK293T cells using previously established isotopic desthiobiotin-ABPP (isoDTB-ABPP).[30] We found that EN884 significantly engaged C160 on SKP1 by 7% (Figure 2e; Table S2). This minimal engagement observed with our covalent SKP1 recruiter is consistent with minimal engagement observed with other covalent E3 ligase recruiters that have been deployed in PROTAC applications, including for DCAF16, DCAF11, and RNF114.[7,8,11] This low degree of engagement is also consistent with EN884 potentially only engaging with a subset of SKP1 in the cell that is engaged with certain CUL1 substrate receptors. We also performed a pulldown proteomics experiment with the SJH1−37m probe and demonstrated 2.8-fold and statistically significant enrichment of SKP1 over vehicle-treated controls (Figure S4c; Table S3). The covalent hit is not yet selective with 414 other targets significantly

https://doi.org/10.1021/acschembio.3c00642
ACS Chem. Biol. XXXX, XXX, XXX−XXX

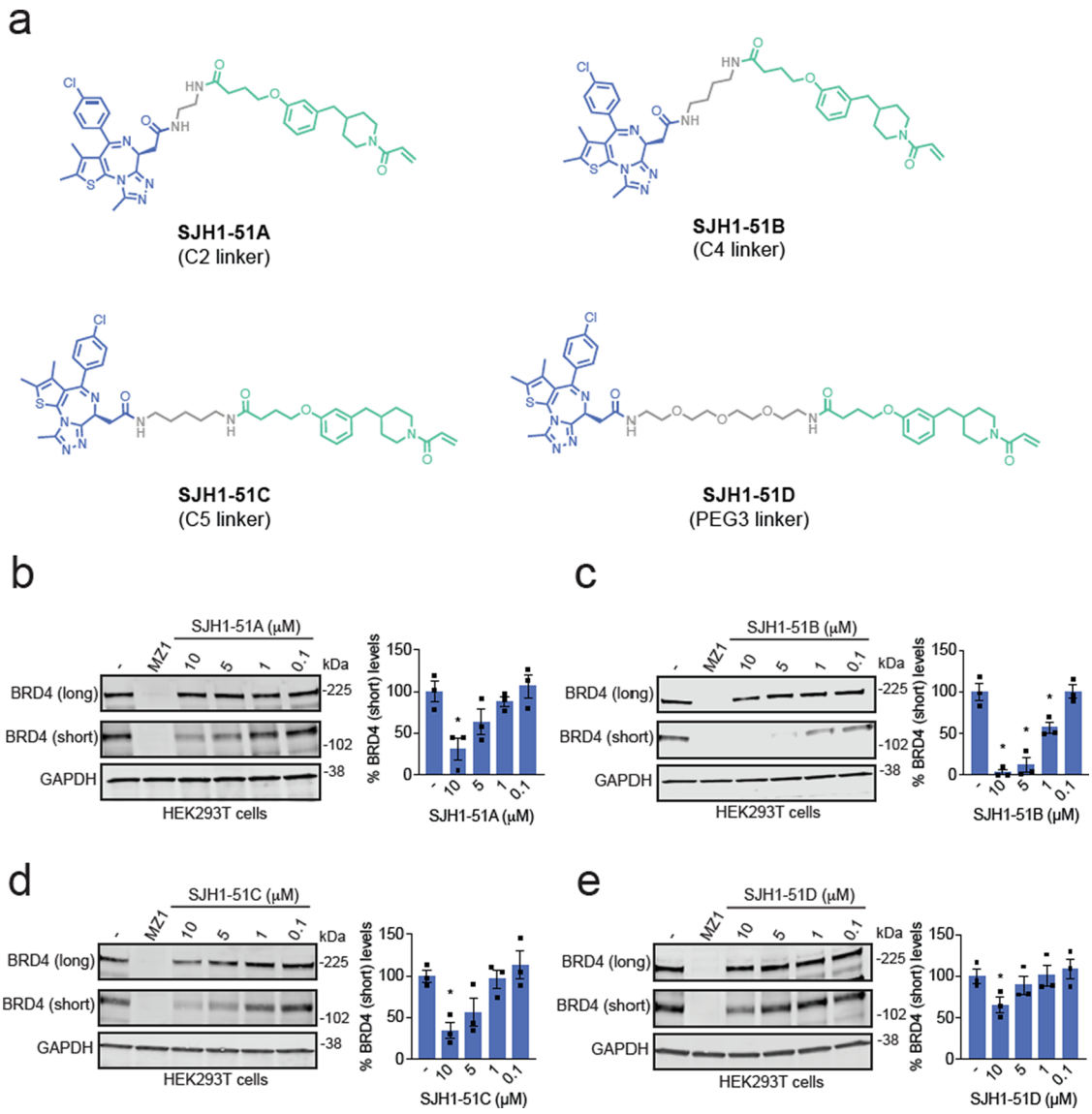

Figure 3. SKP1-based BRD4 degraders. (a) Structures of 4 BRD4 degraders using covalent SKP1 recruiters in green linked via a linker in gray to the BET family inhibitor JQ1 in blue via a C2, C4, or C5 alkyl linker or PEG3 linker. (b−e) BRD4 degradation in cells. HEK293T cells were treated with DMSO vehicle, MZ1 (1 μM), or each degrader for 24 h. The long and short isoforms of BRD4 and loading control GAPDH were assessed by Western blotting, and bands were quantified by densitometry and normalized to GAPDH. Blots are representative of $n = 3$ biologically independent replicates/group. Bar graphs show average ± sem and individual replicate values of the BRD4 short isoform. Significance is expressed as $^*p < 0.05$ compared to vehicle-treated controls.

enriched among 5928 proteins identified, but there were no other proteins involved in the CUL1 E3 ligase complex pulled down by SJH1−37m (Table S3).

Using Covalent SKP1 Recruiter in PROTACs to Degrade BRD4. To demonstrate that our covalent SKP1 ligand could be used in PROTAC applications, we synthesized four different PROTACs linking a derivative of EN884 to the BET family inhibitor JQ1 through either a C2, C4, C5, or PEG3 linker to generate SJH1−51A, SJH1−51B, SJH1−51C, and SJH1−51D, respectively (Figure 3a). All four PROTACs degraded the short, but not long isoform, of BRD4 in HEK293T cells with the most robust degradation observed with SJH1−51B with a C4 alkyl linker (Figure 3b−e). While we observed short isoform-selective BRD4 degradation in HEK293T cells, both isoforms were degraded by SJH1−51B in MDA-MB-231 breast cancer cells, suggesting that this isoform-selective degradation is more of a cell-specific phenomenon rather than the inability to form a productive ternary complex with the long BRD4 isoform (Figure 4a). Tandem mass tagging (TMT)-based quantitative proteomic profiling of SJH1−51B in MDA-MB-231 cells showed moderately selective BRD4 degradation with 16 proteins significantly reduced in levels by >50% (Figure 4b; Table S4).

Consistent with proteasome-mediated degradation, SJH1−51B-mediated BRD4 degradation was attenuated by pretreatment with the proteasome inhibitor bortezomib (Figure 4c). We also showed dependence on NEDDylation required for active Cullin-RING E3 ligases with attenuation of BRD4 degradation by the NEDDylation inhibitor MLN4924 (Figure 4d). Most importantly, we demonstrated that SKP1 knockdown completely attenuated BRD4 degradation by SJH1−51B in HEK293T cells (Figure 4e). Interestingly, we showed that the nonreactive derivative of SJH1−51B, SJH1−51B-NC, was still capable of partially degrading the short isoform of BRD4

https://doi.org/10.1021/acschembio.3c00642
ACS Chem. Biol. XXXX, XXX, XXX−XXX

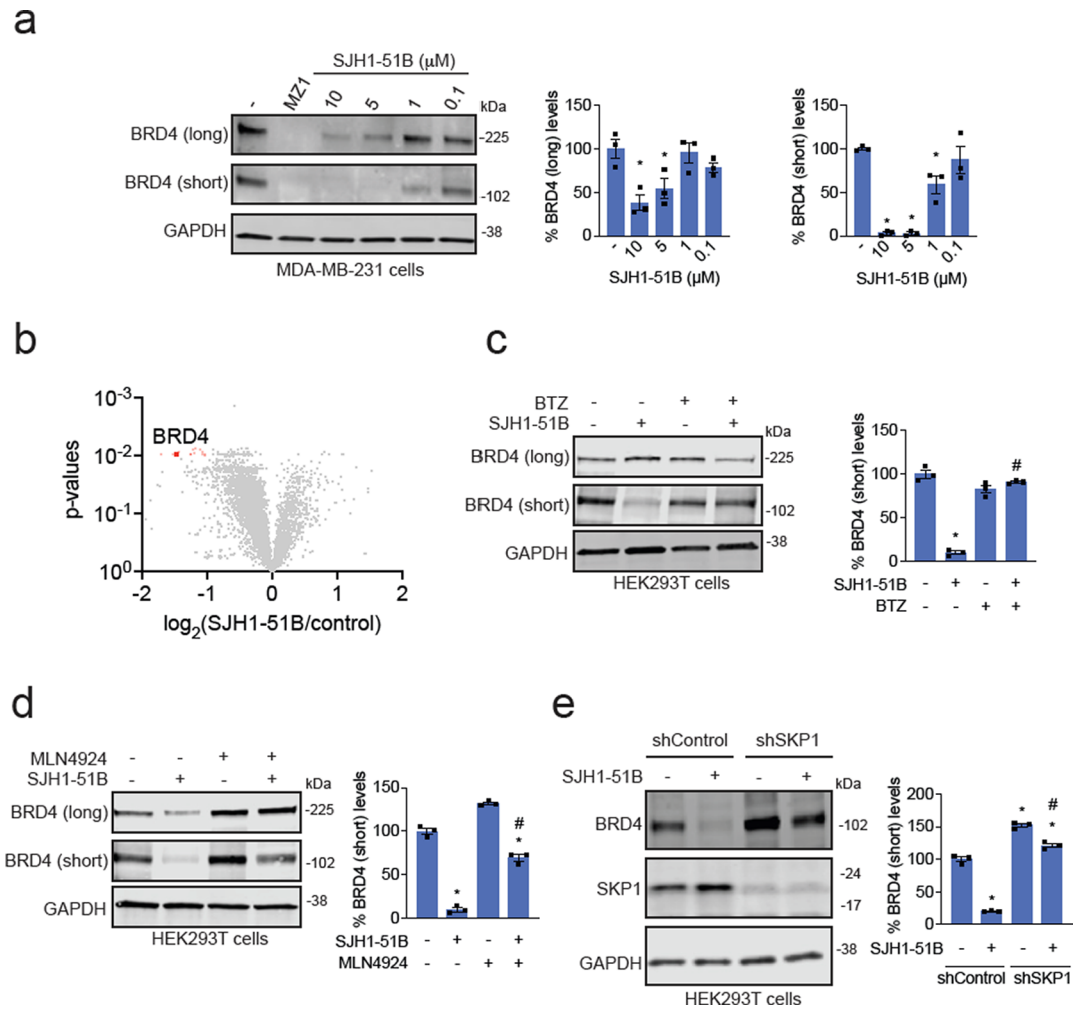

Figure 4. Characterization of BRD4 degrader. (a) BRD4 degradation in MDA-MB-231 cells. MDA-MB-231 cells were treated with DMSO vehicle, MZ1 (1 μM), or SJH1−51B for 24 h. The long and short isoforms of BRD4 and loading control GAPDH were assessed by Western blotting, and bands were quantified by densitometry and normalized to GAPDH. (b) TMT-based quantitative proteomic profiling of SJH1−51B in MDA-MB-231 cells. MDA-MB-231 cells were treated with DMSO vehicle or SJH1−51B (10 μM) for 24 h. Proteomics data can be found in Table S4. (c, d) Proteasome and NEDDylation-dependence of BRD4 degradation. HEK293T cells were pretreated with DMSO vehicle or bortezomib (1 μM) in (c) or MLN4924 (1 μM) in (d) for 1 h prior to treatment of cells with DMSO vehicle or SJH1−51B (10 μM) for 24 h. BRD4 and loading control GAPDH levels were assessed by Western blotting and quantified. (e) Attenuation of BRD4 degradation by SKP1 knockdown. shControl and shSKP1 HEK293T cells were treated with DMSO vehicle or SJH1−51B (5 μM) for 24 h. Short BRD4 isoform, SKP1, and loading control GAPDH levels were assessed by Western blotting and quantified. Blots in (a, c, d, e) are representative of $n = 3$ biologically independent replicates/group. Bar graphs show average ± sem and individual replicate values of BRD4 levels. Significance is expressed as $^*p < 0.05$ compared to vehicle-treated controls, and $\#p < 0.05$ compared to either SJH1−51B treatment alone in (c, d) or compared to SJH1−51B-treated shControl cells in (e).

in HEK293T cells (Figure S5a−c). A comparative time-course of BRD4 degradation with SJH1−51B and SJH1−51B-NC showed degradation of the short isoform of BRD4 short isoform starting at 4−6 h with progressive BRD4 loss through 24 h with 94% versus 42% of BRD4 degraded by the covalent versus the noncovalent degraders at 24 h, respectively (Figure S5d,e). Interestingly, while SJH1−51B and SJH1−51B-NC are clearly based on early stage fragment screening hits, both the covalent SJH1−51B and noncovalent SJH1−51B-NC showed equivalent binding to SKP1 in the Cullin complex by gel-based ABPP, suggesting that these ligands possess appreciable reversible binding affinity for SKP1 (Figure S6a,b). Akin to what we observed with EN884 and SJH1−37m, we did not observe binding of either compound to SKP1 alone (Figure S6b,c). We thus attribute BRD4 degradation observed with the noncovalent PROTAC to its ability to still engage SKP1. The slower degradation rate of BRD4 with the noncovalent PROTAC is likely because of slower binding kinetics to SKP1 or the slower formation of ternary complex compared to the covalent PROTAC.

We also tested established BRD4 PROTACs dBET1 and MZ1 based on cereblon and VHL recruiters in the same MDA-MB-231 background as where we tested our SJH1−51B PROTAC. Given that dBET1 and MZ1 have undergone significant optimization, we expectedly observed that dBET1 and MZ1 more potently and completely degrade BRD4 compared to SJH1−51B (Figure S6c,d).

Using Covalent SKP1 Recruiter in PROTACs to Degrade Androgen Receptor. BRD4 is a relatively easy protein to degrade with PROTACs. As such, we next tested whether our covalent SKP1 recruiter could be used to degrade another neo-substrate protein—the androgen receptor (AR). We synthesized four AR PROTACs linking our covalent SKP1 recruiter to the Arvinas AR PROTAC-targeting ligand from

https://doi.org/10.1021/acschembio.3c00642
ACS Chem. Biol. XXXX, XXX, XXX−XXX

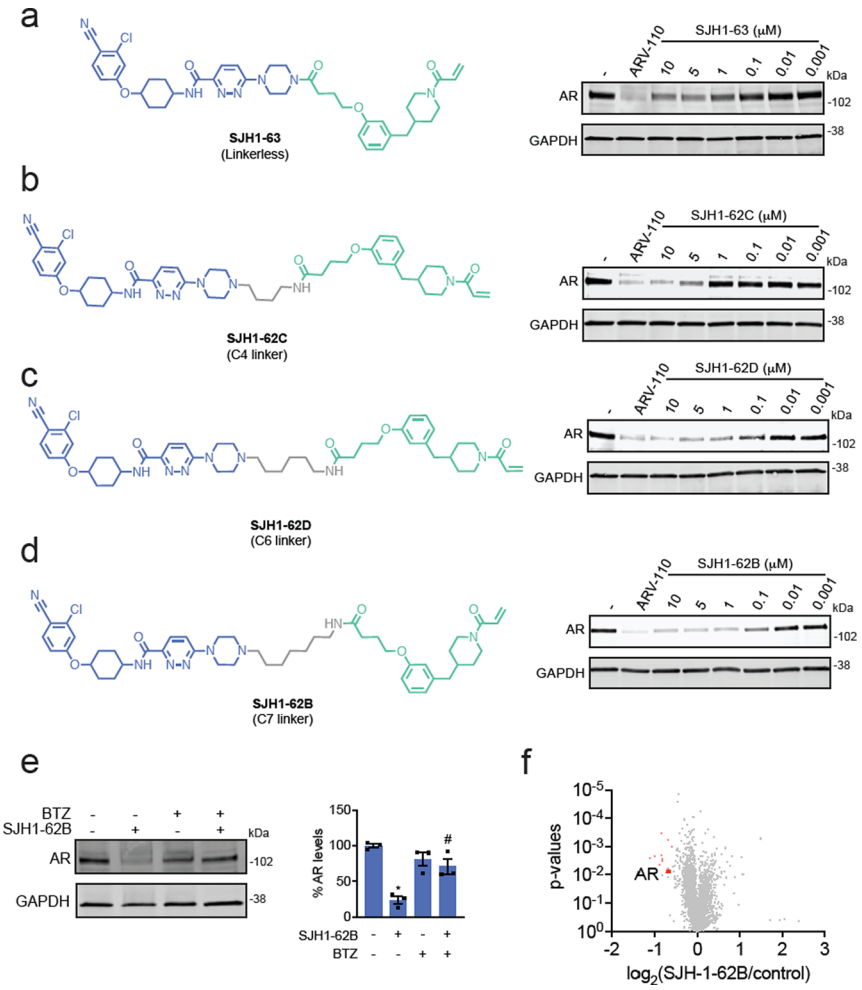

Figure 5. SKP1-based androgen receptor (AR) degraders. (a–d) Structures of AR degraders consisting of SKP1 covalent recruiters in green, linker in gray, and an AR-targeting ligand from ARV-110 in blue with either no linker or C4, C6, or C7 alkyl linkers. Also shown are AR degradation by each degrader in LNCaP prostate cancer cells. LNCaP cells were treated with DMSO vehicle, ARV-110 (1 μM), or each degrader for 24 h. AR and loading control GAPDH levels were assessed by Western blotting. All blots are representative of $n = 3$ biologically independent replicates/group and are quantified in Figure S7. (e) Proteasome dependence of BRD4 degradation. LNCaP cells were pretreated with DMSO vehicle or bortezomib (1 μM) for 1 h prior to treatment of cells with DMSO vehicle or SJH1−62B (1 μM) for 24 h. AR and loading control GAPDH levels were assessed by Western blotting and quantified. Bar graph shows individual replicate values and average ± sem with significance shown as $^{*}p < 0.05$ compared to vehicle-treated controls and $\#p < 0.05$ compared to SJH1−62B treatment alone. (f) TMT-based quantitative proteomic profiling of SJH1−62B in LNCaP cells. LNCaP cells were treated with DMSO vehicle or SJH1−62B (1 μM) for 24 h. Data are from $n = 3$ biologically independent replicates per group, and proteomics data can be found in Table S5.

ARV-110 with either no linker or a C4, C6, or C7 alkyl linker to yield SJH1−63, SJH1−62C, SJH1−62D, and SJH1−62B, respectively (Figure 5a–d).[31] We observed significant AR degradation with all four PROTACs, wherein SJH1−62B with the C7 alkyl linker showed the most potent and robust AR degradation in LNCaP prostate cancer cells (Figure 5a–d; **quantified in** Figure S7). We attempted to show attenuation of AR degradation with SKP1 knockdown or with NEDDylation inhibitors, but even acute SKP1 knockdown with either transient short interfering RNA or lentivirally mediated short hairpin RNA was acutely lethal to LNCaP prostate cancer cells, and MLN4924 treatment alone dramatically lowered AR protein levels (data not shown). As such, we were not able to perform these mechanistic experiments. However, we still demonstrated that SJH1−62B-mediated loss of AR was proteasome-dependent (Figure 5e). Quantitative proteomic profiling also demonstrated relatively selective degradation of AR with 11 other proteins also significantly lowered in levels among >5000 proteins quantified (Figure 5f; Table S5). We synthesized a nonreactive analogue of SJH1−62B, SJH1−62B-NC, and surprisingly observed equivalent AR degradation as SJH1−62B in LNCaP cells with similar degradation kinetics (Figure S8a–e). As was observed with the BRD4 degraders, we found that both SJH1−62B and SJH1−62B-NC both bound equally to SKP1 in the SKP1-FBXO7-CUL1-RBX1 complex, but not or only modestly to SKP1 alone (Figure S9a,b). We also tested the established clinical candidate ARV-110 AR PROTAC in LNCaP cells and demonstrated potent and robust AR degradation (Figure S9c). While ARV-110 showed more robust AR degradation than our SJH1−62B PROTAC, we observed comparable potency of AR degradation.

CONCLUSIONS

Here, we discovered a SKP1 recruiter that covalently targets an intrinsically disordered C160 of SKP1 that sits at the interface of SKP1 and the CUL1 F-box substrate receptor. This

https://doi.org/10.1021/acschembio.3c00642
ACS Chem. Biol. XXXX, XXX, XXX−XXX

observation represents a proof of concept for discovering ligandable sites that exclusively emerge when an IDR containing protein forms a complex with its interacting protein. We further demonstrated that this covalent SKP1 ligand can be used in PROTAC applications to degrade neo-substrates such as BRD4 and AR in cells. Given the essentiality of SKP1, covalent recruitment of SKP1 may potentially overcome resistance mechanisms of PROTACs that utilize nonessential E3 ligases in cancer treatment.

While we demonstrate proof-of-concept of using Cullin-RING E3 ligase adaptor proteins in PROTACs, our SKP1 ligand is still an early hit and will require significant medicinal chemistry optimization to improve potency, selectivity, and druglike properties. By chemoproteomic profiling, we show that EN884 or AD-5−49-based alkyne-functionalized probes still possess a relatively large number of off-targets, and further optimization will need to be done to improve the potency of these compounds while minimizing these off-targets. Intriguingly, we observed that both the covalent and noncovalent BRD4 and AR PROTACs bound to SKP1 in the SKP1-FBXO7-CUL1-RBX1 complex, suggesting that the SKP1 ligand may be a reversible binding component. We also observed both BRD4 and AR degradation with the nonreactive degraders. Future structural biology studies and kinetic studies of ternary complex formation with the covalent and non-covalent degraders will be of value in further optimization of SKP1-based PROTACs. Nonetheless, SKP1 represents another core component of the ubiquitin-proteasome machinery that can be exploited to degrade neo-substrate proteins. Other recently published examples include direct recruitment of the proteasome, recruitment of E2 ubiquitin conjugating enzymes such as UBE2D, as well as the CUL4 adaptor protein DDB1. Our results also highlight the utility of using covalent chemoproteomic approaches to identify recruiters for proteins within the ubiquitin-proteasome system that can be utilized for targeted protein degradation applications.

METHODS

Covalent Ligand Library. Compound names that start with "EN" were purchased from Enamine.

Gel-Based ABPP. Recombinant human SKP1/FBXO7/CUL1/RBX1 complex protein, CF (Boston Biochem, E3−526) was employed for the initial Gel-Based ABPP screening. The SKP1 containing the SCF complex was reconstituted by utilizing a stoichiometric amount of the following recombinant proteins: Recombinant human CUL1/RBX1 Neddylated complex protein (R&D systems, E3−411−025), recombinant human FBXO7 GST (N-Term) protein (Novus Biologicals, H00025793−P01−2ug) or human recombinant FBXO2 protein (Novus Biologicals, NBP2517640.05MG), and recombinant human SKP1 (Bristol Myers Squibb). SKP1 or SKP1 containing SCF complex (0.1 μg) in phosphate-buffered saline (PBS) was incubated with a covalent ligand (50 μM) or DMSO vehicle. After incubating at 23 °C for 1 h, 0.1 μM IA-rhodamine (Setareh Biotech, 6222) was subsequently added. The reaction mixture was incubated at 23 °C for an additional 30 min and quenched by adding 4× reducing Laemmli SDS sample loading buffer (Thermo Scientific, J160015.AD). Samples were boiled at 95 °C for 5 min and separated on precast 4−20% Criterion TGX gels (Bio-Rad). The competition of IA-rhodamine was analyzed by in-gel fluorescent signal using a ChemiDoc MP (Bio-Rad). Imaged gels were stained using Pierce Silver Stain Kit (Thermo Scientific, 24612) following manufacturer's instruction.

Cell Culture. HEK293T, LNCaP, and MDA-MB-231 cell lines were sourced from the UC Berkeley Cell Culture Facility. HEK293T and MDA-MB-231 cells were cultured in Dulbecco's modified Eagle medium supplemented with 10% (v/v) fetal bovine serum (FBS) and 2.5 mM Gibco L-Glutamine (Q). LNCaP cells were cultured using Roswell Park Memorial Institute 1640 medium with 10% (v/v) FBS and 2.5 mM Q. All cells were maintained in a standard incubation environment maintaining 37 °C with 5% CO_2.

Preparation of Cell Lysates. Cells were gently washed with cold PBS twice and subsequently scraped. The scraped cells were pelleted by centrifugation (1400g, 4 min, 4 °C). After removing the supernatant, the pelleted cells were resuspended in PBS containing protease inhibitor (cOmplete, EDTA-free protease inhibitor cocktail). Cells lysis was achieved via sonication, and cellular debris was separated using centrifugation (7500g, 10 min, 4 °C). Cell lysates were then transferred to new tubes, and the concentration of proteome was determined using Pierce BCA protein assay kits (Thermo Scientific, 23227). Next, the cell lysates were further diluted to appropriate experiment condition. For the Western blotting experiments, the pelleted scraped cells were redissolved in the lysis buffer (Thermo Scientific, 89900). After incubating at 4 °C for 30 min with occasional vertexing, the cellular debris was pelleted by centrifugation (7500g, 10 min, 4 °C). The supernatant was collected, and the proteome concentration was verified using BCA assay and further diluted to match the required experimental conditions.

Western Blotting. Proteins were separated by precast 4−20% Criterion TGX gels (Bio-Rad) and transferred to the nitrocellulose membrane using the Trans-Blot Turbo transfer system (Bio-Rad). After the transfer, the membrane was blocked with Tris-buffered saline containing Tween 20 (TBST) containing 5% bovine serum albumin (BSA) for 2 h at 23 °C. After the blocking, targeted proteome was probed with the primary antibody in TBST with 5% BSA (Primary antibody dilution condition from manufacturer). Incubation with the primary antibody was performed overnight (10 h) in a cold room (4 °C), and the primary antibody was washed three times with TBST. The membrane was then incubated in the dark with IR680 or IR800-conjugated secondary antibodies (1:10,000 dilution). After 1 h of incubation at 23 °C, the blot was washed three times with TBST, and the blots were visualized using an Odyssey Li-Cor fluorescent scanner. The following antibodies were used for this study: GAPDH (Proteintech, 60004−1−1G-150L), BRD4 (Abcam, ab128874), androgen receptor (Abcam, ab133273), and SKP1 (Millipore-Sigma, SAB5300376−100UL).

Pulldown of SKP1 Using SJH1−37m. HEK293T cells at 80% confluency were treated with DMSO and SJH1−37m (50 μM). After 4 h of incubation, the cells were harvested, and lysates were prepared as previously described. Each lysate was normalized to a concertation of 5 mg mL^{-1}, and 500 μL of each lysate was transferred to a separate tube. To each tube containing 500 μL of cell lysate, 10 μL of 20 mM biotin picolyl azide (Sigma-Aldrich, 900912) in DMSO, 10 μL of 50 mM TCEP in H_2O, 10 μL of 50 mM $CuSO_4$ in H_2O, and 30 μL of TBTA ligand (1.3 mg mL^{-1} in 1:4 DMSO/tBuOH, Cayman chemical, 18816) were added. The reaction mixture was incubated at 23 °C for 90 min, and the reaction was quenched by protein precipitation. After washing the protein pellets twice with cold MeOH (4 °C), the pellets were redissolved in 200 μL of 1.2% SDS/PBS (w/v). After heating the samples at 95 °C for 10 min, 10 μL of each sample was set aside for the Western blot analysis (input control). One mL of PBS was added to the remaining sample to reduce the total SDS concentration to less than 0.2% SDS/PBS (w/v).

100 μL of streptavidin agarose beads (ThermoFisher, 20353) were added to the lysates containing tubes, and the samples were incubated at 4 °C on a rotator for 10 h. After incubation, the samples were brought to 23 °C, and the beads were spined down in a centrifuge (1300g, 2 min). The supernatant was removed, and the beads were washed three more times with 500 μL of PBS and 500 μL of H_2O. The beads were then suspended in 30 μL of Laemmli SDS sample loading buffer and heated to 95 °C for 10 min. Along with the input control, the resulting samples were subjected to Western blot analysis.

Mapping of EN884 Site of Modification on SKP1 SCF Complex by LC-MS/MS. SKP1 containing SCF complex (100 μg, reconstituted as described) was diluted in PBS (100 μL) and incubated with EN884 (50 μM) for 90 min at 37 °C. The protein was

https://doi.org/10.1021/acschembio.3c00642
ACS Chem. Biol. XXXX, XXX, XXX−XXX

then precipitated by adding 900 μL of acetone, and the precipitation continued at −20 °C for 2 h. The sample was pelleted at 20,000 g for 10 min, 4 °C, and the supernatant was carefully aspirated. The precipitated pellet was washed with 200 μL of acetone. The sample was then resuspended in 30 μL of 8 M urea and 30 μL of ProteaseMax surfactant (20 μg/mL in 100 mM ammonium bicarbonate, Promega, V2071).

After vigorous mixing for 30 s, 40 μL of 100 mM ammonium bicarbonate buffer was added. To the sample containing tube, 10 μL of 110 mM TCEP in H_2O was added, and the sample was incubated at 60 °C for 30 min. Next, 10 μL of 150 mM iodoacetamide in H_2O was added, and the sample was incubated at 37 °C for 30 min. The resulting sample was diluted with 120 μL of PBS containing 1.2 μL of ProteaseMax surfactant (0.1 mg mL^{-1} in 100 mM ammonium bicarbonate). Treated proteins were then digested with sequencing grade modified trypsin (Promega, V5111) and incubated overnight (37 °C, 14 h). Digestion was quenched at the following day by adding 25 μL of formic acid, and the sample was fractionated using high pH reversed-phase peptide fractionation kits (ThermoFisher, 84688) following manufacturer's recommendation.

IsoDTB-ABPP Cysteine Chemoproteomic Profiling and TMT Proteomic Profiling Methods. Methods are described in the Supporting Information.

■ ASSOCIATED CONTENT

Supporting Information

The Supporting Information is available free of charge at https://pubs.acs.org/doi/10.1021/acschembio.3c00642.

Primary SKP1 screen, site of modification analysis of SKP1 ligand against SKP1, structural analysis of SKP1, structure−activity relationship of EN884 analogues for SKP1 binding, chemoproteomic profiling of SJH1−37m, characterization of nonreactive BRD4 and AR degraders, quantification of blots, synthetic methods and characterization of compounds, and NMR spectra of compounds synthesized in this study (PDF)

Compounds screened (XLSX)

isoDTB-ABPP (XLSX)

SJH1-37m pulldown TMT (XLSX)

BRD4 PROTAC (XLSX)

AR PROTAC TMT (XLSX)

■ AUTHOR INFORMATION

Corresponding Author

Daniel K. Nomura − *Department of Chemistry and Department of Molecular and Cell Biology, University of California, Berkeley, Berkeley, California 94720, United States; Innovative Genomics Institute, Berkeley, California 94720, United States;* orcid.org/0000-0003-1614-8360; Email: dnomura@berkeley.edu

Authors

Seong Ho Hong − *Department of Chemistry, University of California, Berkeley, Berkeley, California 94720, United States; Innovative Genomics Institute, Berkeley, California 94720, United States;* orcid.org/0000-0002-8634-452X

Anand Divakaran − *Department of Chemistry, University of California, Berkeley, Berkeley, California 94720, United States; Innovative Genomics Institute, Berkeley, California 94720, United States*

Akane Osa − *Department of Chemistry, University of California, Berkeley, Berkeley, California 94720, United States; Innovative Genomics Institute, Berkeley, California 94720, United States*

Oscar W. Huang − *Bristol Myers Squibb, Redwood City, California 94063, United States*

Ingrid E. Wertz − *Bristol Myers Squibb, Redwood City, California 94063, United States*

Complete contact information is available at: https://pubs.acs.org/10.1021/acschembio.3c00642

Author Contributions

S.H.H., D.K.N., and I.E.W. conceived the project idea. S.H.H., A.D., and D.K.N. designed the experiments, performed the experiments, analyzed and interpreted the data, and wrote the paper. S.H.H., A.D., D.K.N., A.O., and O.W.H. performed the experiments, analyzed and interpreted data, and provided intellectual contributions. S.H.H. and A.D. contributed equally to this manuscript.

Notes

The authors declare the following competing financial interest(s): IEW was an employee of Bristol Myers Squibb when this study was initiated but is now an employee of Lyterian. DKN is a co-founder, shareholder, and scientific advisory board member for Frontier Medicines and Vicinitas Therapeutics. DKN is a member of the board of directors for Vicinitas Therapeutics. DKN is also on the scientific advisory board of The Mark Foundation for Cancer Research, Photys Therapeutics, and Apertor Pharmaceuticals. DKN is also an Investment Advisory Partner for a16z Bio, an Advisory Board member for Droia Ventures, and an iPartner for The Column Group.

■ ACKNOWLEDGMENTS

We thank the members of the Nomura Research Group and Bristol Myers Squibb for critical reading of the manuscript. This work was supported by Bristol Myers Squibb for all listed authors. This work was also supported by the Nomura Research Group and The Mark Foundation for Cancer Research ASPIRE Award for D.K.N. and The Mark Foundation for Cancer Research Momentum Fellowship for A.D. This work was also supported by grants from the National Institutes of Health (R01CA240981 and R35CA263814 for D.K.N.) and the National Science Foundation Molecular Foundations for Biotechnology Award (2127788). We also thank H Celik and UC Berkeley's NMR facility in the College of Chemistry (CoC-NMR) for spectroscopic assistance. Instruments in the College of Chemistry NMR facility are supported in part by NIH S10OD024998.

■ REFERENCES

(1) Belcher, B. P.; Ward, C. C.; Nomura, D. K. Ligandability of E3 Ligases for Targeted Protein Degradation Applications. *Biochemistry* **2023**, *62* (3), 588−600.

(2) Buckley, D. L.; Van Molle, I.; Gareiss, P. C.; Tae, H. S.; Michel, J.; Noblin, D. J.; Jorgensen, W. L.; Ciulli, A.; Crews, C. M. Targeting the von Hippel-Lindau E3 Ubiquitin Ligase Using Small Molecules to Disrupt the VHL/HIF-1α Interaction. *J. Am. Chem. Soc.* **2012**, *134* (10), 4465−4468.

(3) Zengerle, M.; Chan, K.-H.; Ciulli, A. Selective Small Molecule Induced Degradation of the BET Bromodomain Protein BRD4. *ACS Chem. Biol.* **2015**, *10* (8), 1770−1777.

(4) Winter, G. E.; Buckley, D. L.; Paulk, J.; Roberts, J. M.; Souza, A.; Dhe-Paganon, S.; Bradner, J. E. DRUG DEVELOPMENT. Phthalimide Conjugation as a Strategy for in Vivo Target Protein Degradation. *Science* **2015**, *348* (6241), 1376−1381.

(5) Okuhira, K.; Demizu, Y.; Hattori, T.; Ohoka, N.; Shibata, N.; Nishimaki-Mogami, T.; Okuda, H.; Kurihara, M.; Naito, M.

Development of Hybrid Small Molecules That Induce Degradation of Estrogen Receptor-Alpha and Necrotic Cell Death in Breast Cancer Cells. *Cancer Sci.* **2013**, *104* (11), 1492−1498.
(6) Hines, J.; Lartigue, S.; Dong, H.; Qian, Y.; Crews, C. M. MDM2-Recruiting PROTAC Offers Superior, Synergistic Antiproliferative Activity via Simultaneous Degradation of BRD4 and Stabilization of P53. *Cancer Res.* **2019**, *79* (1), 251−262.
(7) Zhang, X.; Crowley, V. M.; Wucherpfennig, T. G.; Dix, M. M.; Cravatt, B. F. Electrophilic PROTACs That Degrade Nuclear Proteins by Engaging DCAF16. *Nat. Chem. Biol.* **2019**, *15* (7), 737−746.
(8) Zhang, X.; Luukkonen, L. M.; Eissler, C. L.; Crowley, V. M.; Yamashita, Y.; Schafroth, M. A.; Kikuchi, S.; Weinstein, D. S.; Symons, K. T.; Nordin, B. E.; Rodriguez, J. L.; Wucherpfennig, T. G.; Bauer, L. G.; Dix, M. M.; Stamos, D.; Kinsella, T. M.; Simon, G. M.; Baltgalvis, K. A.; Cravatt, B. F. DCAF11 Supports Targeted Protein Degradation by Electrophilic Proteolysis-Targeting Chimeras. *J. Am. Chem. Soc.* **2021**, *143* (13), 5141−5149.
(9) Tao, Y.; Remillard, D.; Vinogradova, E. V.; Yokoyama, M.; Banchenko, S.; Schwefel, D.; Melillo, B.; Schreiber, S. L.; Zhang, X.; Cravatt, B. F. Targeted Protein Degradation by Electrophilic PROTACs That Stereoselectively and Site-Specifically Engage DCAF1. *J. Am. Chem. Soc.* **2022**, *144* (40), 18688−18699.
(10) Vulpetti, A.; Holzer, P.; Schmiedeberg, N.; Imbach-Weese, P.; Pissot-Soldermann, C.; Hollingworth, G. J.; Radimerski, T.; Thoma, C. R.; Stachyra, T.-M.; Wojtynek, M.; Maschlej, M.; Chau, S.; Schuffenhauer, A.; Fernández, C.; Schröder, M.; Renatus, M. Discovery of New Binders for DCAF1, an Emerging Ligase Target in the Targeted Protein Degradation Field. *ACS Med. Chem. Lett.* **2023**, *14* (7), 949−954.
(11) Spradlin, J. N.; Hu, X.; Ward, C. C.; Brittain, S. M.; Jones, M. D.; Ou, L.; To, M.; Proudfoot, A.; Ornelas, E.; Woldegiorgis, M.; Olzmann, J. A.; Bussiere, D. E.; Thomas, J. R.; Tallarico, J. A.; McKenna, J. M.; Schirle, M.; Maimone, T. J.; Nomura, D. K. Harnessing the Anti-Cancer Natural Product Nimbolide for Targeted Protein Degradation. *Nat. Chem. Biol.* **2019**, *15* (7), 747−755.
(12) Luo, M.; Spradlin, J. N.; Boike, L.; Tong, B.; Brittain, S. M.; McKenna, J. M.; Tallarico, J. A.; Schirle, M.; Maimone, T. J.; Nomura, D. K. Chemoproteomics-Enabled Discovery of Covalent RNF114-Based Degraders That Mimic Natural Product Function. *Cell Chem. Biol.* **2021**, *28* (4), 559−566.e15.
(13) Henning, N. J.; Manford, A. G.; Spradlin, J. N.; Brittain, S. M.; Zhang, E.; McKenna, J. M.; Tallarico, J. A.; Schirle, M.; Rape, M.; Nomura, D. K. Discovery of a Covalent FEM1B Recruiter for Targeted Protein Degradation Applications. *J. Am. Chem. Soc.* **2022**, *144* (2), 701−708.
(14) Ward, C. C.; Kleinman, J. I.; Brittain, S. M.; Lee, P. S.; Chung, C. Y. S.; Kim, K.; Petri, Y.; Thomas, J. R.; Tallarico, J. A.; McKenna, J. M.; Schirle, M.; Nomura, D. K. Covalent Ligand Screening Uncovers a RNF4 E3 Ligase Recruiter for Targeted Protein Degradation Applications. *ACS Chem. Biol.* **2019**, *14* (11), 2430−2440.
(15) Tong, B.; Luo, M.; Xie, Y.; Spradlin, J. N.; Tallarico, J. A.; McKenna, J. M.; Schirle, M.; Maimone, T. J.; Nomura, D. K. Bardoxolone Conjugation Enables Targeted Protein Degradation of BRD4. *Sci. Rep.* **2020**, *10* (1), 15543.
(16) Du, G.; Jiang, J.; Henning, N. J.; Safaee, N.; Koide, E.; Nowak, R. P.; Donovan, K. A.; Yoon, H.; You, I.; Yue, H.; Eleuteri, N. A.; He, Z.; Li, Z.; Huang, H. T.; Che, J.; Nabet, B.; Zhang, T.; Fischer, E. S.; Gray, N. S. Exploring the Target Scope of KEAP1 E3 Ligase-Based PROTACs. *Cell Chem. Biol.* **2022**, *29* (10), 1470−1481.e31.
(17) Ottis, P.; Palladino, C.; Thienger, P.; Britschgi, A.; Heichinger, C.; Berrera, M.; Julien-Laferriere, A.; Roudnicky, F.; Kam-Thong, T.; Bischoff, J. R.; Martoglio, B.; Pettazzoni, P. Cellular Resistance Mechanisms to Targeted Protein Degradation Converge Toward Impairment of the Engaged Ubiquitin Transfer Pathway. *ACS Chem. Biol.* **2019**, *14* (10), 2215−2223.
(18) Zhang, L.; Riley-Gillis, B.; Vijay, P.; Shen, Y. Acquired Resistance to BET-PROTACs (Proteolysis-Targeting Chimeras) Caused by Genomic Alterations in Core Components of E3 Ligase Complexes. *Mol. Cancer Ther.* **2019**, *18* (7), 1302−1311.
(19) Gosavi, P. M.; Ngan, K. C.; Yeo, M. J. R.; Su, C.; Li, J.; Lue, N. Z.; Hoenig, S. M.; Liau, B. B. Profiling the Landscape of Drug Resistance Mutations in Neosubstrates to Molecular Glue Degraders. *ACS Cent. Sci.* **2022**, *8* (4), 417−429.
(20) Baek, K.; Scott, D. C.; Schulman, B. A. NEDD8 and Ubiquitin Ligation by Cullin-RING E3 Ligases. *Curr. Opin. Struct. Biol.* **2021**, *67*, 101−109.
(21) Słabicki, M.; Kozicka, Z.; Petzold, G.; Li, Y.-D.; Manojkumar, M.; Bunker, R. D.; Donovan, K. A.; Sievers, Q. L.; Koeppel, J.; Suchyta, D.; Sperling, A. S.; Fink, E. C.; Gasser, J. A.; Wang, L. R.; Corsello, S. M.; Sellar, R. S.; Jan, M.; Gillingham, D.; Scholl, C.; Fröhling, S.; Golub, T. R.; Fischer, E. S.; Thomä, N. H.; Ebert, B. L. The CDK Inhibitor CR8 Acts as a Molecular Glue Degrader That Depletes Cyclin K. *Nature* **2020**, *585* (7824), 293−297.
(22) Mahon, C.; Krogan, N. J.; Craik, C. S.; Pick, E. Cullin E3 Ligases and Their Rewiring by Viral Factors. *Biomolecules* **2014**, *4* (4), 897−930.
(23) Meyers, M.; Cismoski, S.; Panidapu, A.; Chie-Leon, B.; Nomura, D. K. Targeted Protein Degradation through Recruitment of the CUL4A Complex Adaptor Protein DDB1. *bioRxiv* **2023**, 2023.08.11.553046 DOI: 10.1101/2023.08.11.553046.
(24) Liu, Y.; Patricelli, M. P.; Cravatt, B. F. Activity-Based Protein Profiling: The Serine Hydrolases. *Proc. Natl. Acad. Sci. U. S. A.* **1999**, *96* (26), 14694−14699.
(25) Zheng, N.; Schulman, B. A.; Song, L.; Miller, J. J.; Jeffrey, P. D.; Wang, P.; Chu, C.; Koepp, D. M.; Elledge, S. J.; Pagano, M.; Conaway, R. C.; Conaway, J. W.; Harper, J. W.; Pavletich, N. P. Structure of the Cul1-Rbx1-Skp1-F boxSkp2 SCF Ubiquitin Ligase Complex. *Nature* **2002**, *416* (6882), 703−709.
(26) Hao, B.; Zheng, N.; Schulman, B. A.; Wu, G.; Miller, J. J.; Pagano, M.; Pavletich, N. P. Structural Basis of the Cks1-Dependent Recognition of P27(Kip1) by the SCF(Skp2) Ubiquitin Ligase. *Mol. Cell* **2005**, *20* (1), 9−19.
(27) Kumanomidou, T.; Nishio, K.; Takagi, K.; Nakagawa, T.; Suzuki, A.; Yamane, T.; Tokunaga, F.; Iwai, K.; Murakami, A.; Yoshida, Y.; Tanaka, K.; Mizushima, T. The Structural Differences between a Glycoprotein Specific F-Box Protein Fbs1 and Its Homologous Protein FBG3. *PloS One* **2015**, *10* (10), No. e0140366.
(28) Yalla, K.; Elliott, C.; Day, J. P.; Findlay, J.; Barratt, S.; Hughes, Z. A.; Wilson, L.; Whiteley, E.; Popiolek, M.; Li, Y.; Dunlop, J.; Killick, R.; Adams, D. R.; Brandon, N. J.; Houslay, M. D.; Hao, B.; Baillie, G. S. FBXW7 Regulates DISC1 Stability via the Ubiquitin-Proteosome System. *Mol. Psychiatry* **2018**, *23* (5), 1278−1286.
(29) Mizushima, T.; Yoshida, Y.; Kumanomidou, T.; Hasegawa, Y.; Suzuki, A.; Yamane, T.; Tanaka, K. Structural Basis for the Selection of Glycosylated Substrates by SCF(Fbs1) Ubiquitin Ligase. *Proc. Natl. Acad. Sci. U. S. A.* **2007**, *104* (14), 5777−5781.
(30) Zanon, P. R. A.; Lewald, L.; Hacker, S. M. Isotopically Labeled Desthiobiotin Azide (isoDTB) Tags Enable Global Profiling of the Bacterial Cysteinome. *Angew. Chem., Int. Ed.* **2020**, *59* (7), 2829−2836.
(31) Proof-of-Concept with PROTACs in Prostate Cancer. *Cancer Discovery* **2020**, *10* (8), 1084. .

https://doi.org/10.1021/acschembio.3c00642
ACS Chem. Biol. XXXX, XXX, XXX−XXX